

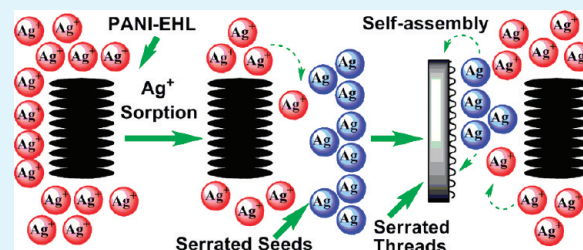
# Facile Preparation of Hierarchical Polyaniline-Lignin Composite with a Reactive Silver-Ion Adsorbability

Zhi-Wei He, Qiu-Feng Lü,\* and Jia-Yin Zhang

College of Materials Science and Engineering, Fuzhou University, 2 Xueyuan Road, Fuzhou 350108, P. R. China

**ABSTRACT:** A hierarchical polyaniline-lignin (PANI-EHL) composite was facilely prepared from aniline and enzymatic hydrolysis lignin in an aqueous solution of ammonia. The morphology, FTIR, UV-vis spectra, thermogravimetric analysis, and wide-angle X-ray diffraction analyses of the composite were systematically investigated. Furthermore, the sorption property of the PANI-EHL composite for silver ions in aqueous solution was studied via a static sorption technique. The result demonstrated that the PANI-EHL composite possessed a strongly reactive sorption characteristic for silver ions. Serrated silver threads with length up to 10 mm were obtained by using the PANI-EHL composite as a low-cost adsorbent. Moreover, the role of EHL and polyaniline in the PANI-EHL composite for silver ions sorption was investigated. The investigation indicated that the EHL unit could play a vital role in the chelation of silver ions, whereas the polyaniline unit played a leading role in redox sorption.

**KEYWORDS:** polyaniline, enzymatic hydrolysis lignin, composite, hierarchical structure, reactive sorption, serrated silver threads



## INTRODUCTION

Silver is one of the most important noble metals because of its wide applications in electronic components,<sup>1</sup> DNA and microRNA detection,<sup>2</sup> luminescent materials,<sup>3</sup> catalysts,<sup>4</sup> antibacterial materials,<sup>5–7</sup> etc. Consequently, excessive industrial wastewater containing silver ions is unavoidable as a result of the widespread use of silver. Such widespread use is anticipated to result in a serious worldwide problem that will endanger the environment and human health. Therefore, various methods<sup>8–10</sup> and adsorbents<sup>8–13</sup> have been employed for the recovery and removal of silver ions from wastewater. Among the applicable methods, sorption of aqueous silver ions has been recognized as the most optimum method because of its high efficiency, ease of implementation, and low cost.

Polyaniline (PANI) and its composite have been applied in the adsorption of Cr(VI),<sup>14–16</sup> Hg(II),<sup>17</sup> Cd(II),<sup>18</sup> Cu(II),<sup>19,20</sup> and dyes.<sup>21,22</sup> Especially, because of the highly reactive sensitivity of the amine and imine functional groups of PANI to silver ions,<sup>23–25</sup> PANI has become a promising adsorbent for waste silver solutions. Furthermore, the silver ions in solution could be reduced to silver through sorption and chemical reduction by PANI due to its three idealized oxidation states.<sup>26,27</sup> This is because the nitrogen atoms not only play a role in chelation but also act on the reduction process at the same time. However, the adsorptive property of the PANI-based adsorbent needs to be further enhanced. Therefore, it is necessary to seek out powerful adsorbents that could be used to obtain large quantities of silver that have been reduced following treatment of waste silver solutions.

Lignin, as a reproducible natural resource, is mainly used as fuel, whereas only a small amount employed in specialty products.<sup>28</sup> However, when lignin is used directly as fuel from

industrial or agricultural waste products it releases large amounts of CO<sub>2</sub>, which plays an important part in the greenhouse effect. In particular, the polycyclic structures with negative groups on the lignin units could play a vital role in chelation, making lignin a promising sorption candidate.<sup>29,30</sup> Compared with other low-cost sorbents, lignin exhibits effective sorption performance for some metal ions including Cr(III),<sup>28</sup> Cu(II),<sup>31</sup> Pb(II), Zn(II),<sup>32</sup> ions, and dyes.<sup>33</sup> Generally, lignin does not react easily with aniline without it first being treated before reaction. However, enzymatic hydrolysis lignin (EHL) is a novel lignin isolated from the enzymatic hydrolysis residues of biomass.<sup>34</sup> Compared with lignin treated by strong physical or chemical methods, such as liginosulfonate and kraft lignin, EHL exhibits high chemical activity and can be used to prepare lignin-based polymers.<sup>35</sup>

The aim of this study was to present the facile fabrication of a low-cost PANI-EHL composite from aniline and EHL in an aqueous solution of ammonia. Furthermore, the PANI-EHL composite was used as a powerful adsorbent of wastewater containing silver ions. In view of the respective advantages of EHL and PANI, the resultant PANI-EHL composite is expected to exhibit an enhanced performance for the sorption of silver ions.

## EXPERIMENTAL SECTION

**Materials.** Aniline was obtained from Sinopharm Chemical Reagent Co. Ltd. (Shanghai, China) and purified by distillation under reduced pressure prior to use. Enzymatic hydrolysis lignin (EHL) made from cornstalk residues, was supplied by Shandong

Received: October 20, 2011

Accepted: November 28, 2011

Published: December 23, 2011

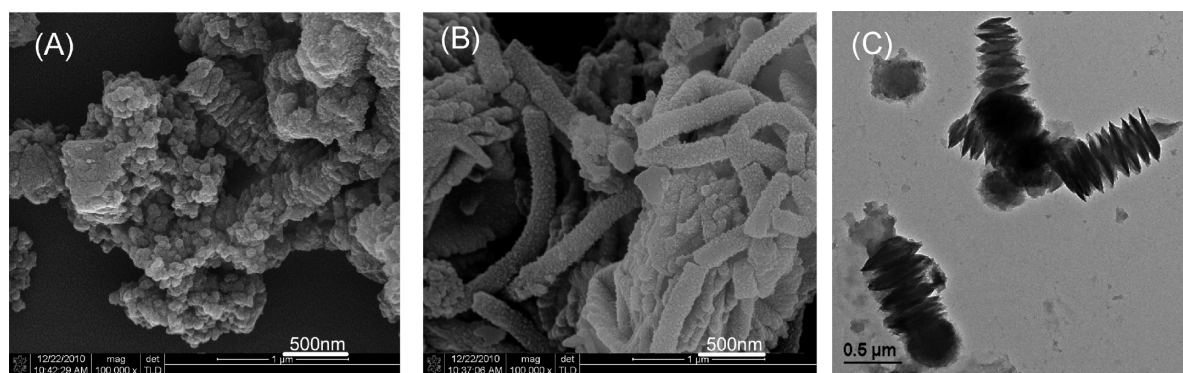


**Figure 1.** (A, B) FE-SEM and (C) TEM images of (A, C) the PANI-EHL composite and (B) PANI.

Longlive Bio-technology Co. Ltd. (Shandong, China), in powder form. Ammonium persulfate (APS), silver nitrate ( $\text{AgNO}_3$ ), ammonia and other solvents were purchased from Sinopharm Chemical Reagent Co. Ltd. (Shanghai, China) and used as received.

**Preparation of Hierarchical PANI-EHL Composite.** A representative polymerization for the PANI-EHL (mass ratio of aniline to EHL = 9:1) composite was as follows: EHL (1.86 g) was dissolved in an aqueous solution of ammonia (0.01 M, 70 mL) in a 150 mL glass flask placed in a 25 °C water bath and stirred vigorously with a magnetic stir bar for 30 min. Then, aniline (1.83 mL, 20 mmol) was added into the EHL solution and stirred vigorously for 30 min to form a mixture of aniline-EHL. Ammonium persulfate (APS, 4.56 g, 20 mmol) was dissolved separately in aqueous solution of ammonia (0.01 M, 30 mL) to prepare an oxidant solution. The APS solution was poured into the aniline-EHL mixture solution at 25 °C. Then, the reaction was carried out at 25 °C in a water bath without any stirring for 24 h. After the reaction, the PANI-EHL composite with hierarchical structures was isolated from the reaction mixture by filtration and washed with an excess amount of aqueous ammonia (0.01 M) solution to remove the residual oxidant, EHL, and water-soluble aniline oligomers. The dark black product remaining was dried in a vacuum oven at 60 °C for 1 week to obtain the PANI-EHL composite powder.

**Silver Ion Sorption.** Sorption of silver ions from aqueous solution using the PANI-EHL composite as an adsorbent was performed in batch experiments. The PANI-EHL composite (50 mg) and  $\text{AgNO}_3$  aqueous solution (50 mM, 25 mL) were added into a 100 mL glass flask. Then, the glass flask was placed in an ultrasonic instrument (200 W) for 5 min to disperse the PANI-EHL composite powder in the  $\text{AgNO}_3$  aqueous solution. After that, the solution was kept in a water bath at 25 °C for a certain sorption period. After a desired sorption period, the PANI-EHL composite was filtrated from the solution. The concentration of silver ions in the filtrate after sorption was measured using the Mohr method. The adsorbed amount of silver on the PANI-EHL composite was calculated according to the following equation.

$$Q = (C_0 - C_i)VM/W \quad (1)$$

where  $Q$  is the sorption capacity (mg/g);  $C_0$  and  $C_i$  are the silver ions' concentration (M) before and after sorption, respectively;  $V$  is the initial volume of the silver ion solution (mL);  $M$  is the molecular weight of silver ions (g/mol); and  $W$  is the weight of the sorbent added (g).

**Characterization.** FTIR spectra were recorded on a Nicolet FTIR 5700 spectrophotometer in KBr pellets. UV-Vis spectra were measured on a Varian Cary50 spectrometer in a wavelength range of 200–800 nm for characterization of the macromolecular structure. Wide-angle X-ray diffraction scans for the samples were obtained using an Ultima III X-ray model diffractometer (Rigaku, Japan) with  $\text{CuK}\alpha$  radiation at a scanning rate of  $10^\circ/\text{min}$  in a reflection mode over a  $2\theta$  range from  $5^\circ$  to  $80^\circ$ . Morphological analysis of the samples was performed using a field emission scanning electron microscopy (FE-SEM, FEI nanoSEM 230) and transmission electron microscopy (TEM, JEM-2010, Jeol), respectively. Thermogravimetric analysis (TGA) curves were recorded

using a SDT-Q600 TGA (TA, USA) in a temperature range of 0–800 °C under a nitrogen flow of 100 mL/min.

## RESULTS AND DISCUSSION

**Morphology.** The PANI-EHL composite was prepared in aqueous ammonia solution because EHL powder is only soluble in alkaline solution. The typical FE-SEM and TEM images of the PANI-EHL composite shown in A and C in Figure 1 clearly reveal hierarchical structures with diameters of about 480 nm. However, PANI (Figure 1B) exhibits tubular structures with diameters of 170 nm. Compared with PANI, the surface of the PANI-EHL composite is much rougher and has more defects because the polycyclic structures with negatively charged carboxyl groups of EHL could help the PANI-EHL composite form the hierarchical structure. Furthermore, in alkaline solution, the protonation of aniline is restrained while neutral aniline monomers become the main object of oxidization,<sup>36–38</sup> which is beneficial to the formation of the hierarchical structure.

**FTIR and UV-vis Spectra.** The preparation of the PANI-EHL composite was carried out at room temperature, which was an apt temperature to form hierarchical structures, where the morphology of the PANI-EHL composite has much to do with the polymerization temperature.<sup>37–39</sup> FTIR and UV-Vis spectra (Figure 2) confirmed that the structures of the PANI-

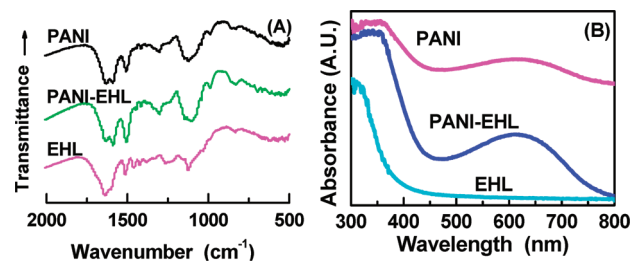


**Figure 2.** (A) FTIR and (B) UV-vis spectra of PANI, the PANI-EHL composite, and EHL.

EHL composite are different to those of PANI and EHL,<sup>16,40–42</sup> implying the existence of an interaction between the PANI and EHL components in the PANI-EHL composite and provides evidence for the formation of the grafted structure of the PANI-EHL composite. On the basis of a recent report on the products of aniline prepared under alkaline conditions, there is also a possibility that an aniline oligomer and PANI coexisted in the PANI-EHL composite.<sup>43</sup> However, as for the PANI-EHL composite, the aniline oligomers were most likely

removed when the composite was washed with an excess of 0.01 M aqueous ammonia solution. The relative intensities of the peaks at 1590, 1300, 1165, 753, and 691  $\text{cm}^{-1}$  also demonstrate that there are no aniline oligomers in the PANI-EHL composite.<sup>43</sup> Moreover, the relative absorption intensities at 1575 and 1140  $\text{cm}^{-1}$  correspond to the extent of oxidation and protonation, respectively,<sup>16,42,44</sup> indicating that the PANI-EHL composite is in the emeraldine salt form. It might be due to the presence of sulfuric acid generated from hydrogen atoms abstracted from aniline and peroxydisulfate. Compared with the UV-vis and FTIR absorption spectra of pure PANI, the absorption spectrum of the PANI-EHL composite showed a little blue shift, indicating that the presence of EHL in the PANI-EHL composite reduces the  $\pi$  conjugation of PANI.<sup>40,41</sup> For this reason, the nitrogen in the PANI-EHL composite is more unstable and is apt to react with silver ion via reactive sorption.

**TGA Analysis.** The TGA curves of EHL, PANI, and the PANI-EHL composite are displayed in Figure 3. The thermal

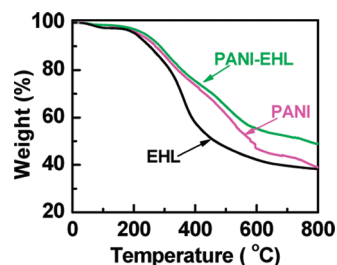


**Figure 3.** TGA curves of PANI, the PANI-EHL composite, and EHL.

degradation stages of the two curves of PANI and the PANI-EHL composite began from about 180 °C and reached the fastest rate at about 350 °C where the rate of weight loss was the fastest. For the curve of EHL, the thermal degradation stage began from about 80 °C and reached the fastest rate at about 350 °C. Compared with the two curves of EHL and PANI, the curve of the PANI-EHL composite was always above that of EHL and PANI, which signified that the thermal stability of the PANI-EHL composite was better than EHL and PANI. A possible interpretation is that there are reactions between the rigidity of the EHL chains and the long PANI chains. Therefore, there should be the existence of an interaction in the PANI-EHL composite, and at least part of the aniline monomers were formed as branches of the PANI-EHL composite. Only in this way can the curve of the PANI-EHL composite, which appears above the two curves of EHL and PANI, be well explained.

**Reactive Sorption of Silver Ion onto the PANI-EHL Composite.** The silver ion sorption capacities of the PANI-EHL composite, PANI and EHL were discussed. The silver ion sorption capacity of PANI and EHL is up to 631 and 285  $\text{mg g}^{-1}$ , respectively, when the silver ion sorption was performed with the initial concentration  $\text{AgNO}_3$  aqueous solution of 50 mM at 25 °C. However, the maximal silver ion sorption capacity of the PANI-EHL composite reached 662  $\text{mg g}^{-1}$  when the PANI-EHL composite was used as an adsorbent (Figure 4). The good adsorbability of silver ion onto the PANI-EHL composite is mainly attributable to the existence of  $-\text{NH}-$ ,  $-\text{N}=\text{}$ , and  $-\text{OCH}_3$  functional groups in the composite chains spread over the rough surface of the sample. However, the silver ion sorption capacity of the PANI-EHL composite is

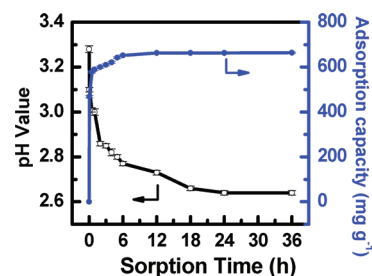


**Figure 4.** Variations in pH value and sorption capacity of the silver ion solutions with sorption time.

lower than that of poly(1,8-diaminonaphthalene)<sup>23</sup> and 4-sulfonic diphenylamine/1,8-diaminonaphthalene copolymer<sup>24</sup> microparticles because the poly(1,8-diaminonaphthalene) chains have much more free amino ( $-\text{NH}_2$ ) groups. Furthermore, the sorption capacity of the PANI-EHL composite is very likely to be influenced by two factors. The first factor is that the increase in oxidized  $-\text{N}=\text{}$  groups newly formed during the powerful reactive silver ions sorption process of the PANI-EHL composite will reduce the sorption capacity of the N groups (Scheme 1A); and a second factor is that the reduced silver nanoparticles on the surface of the hierarchical PANI-EHL composite hinder further sorption of silver ions (Scheme 1B).

Moreover, a sorption product containing serrated silver threads (Figures 5A and B) with length up to 10 mm was achieved from the PANI-EHL composite. The serrated silver threads obtained as a result of the reductibility of the PANI-EHL composite could easily be observed with the naked eyes and measured using a ruler as shown in Figure 5A. However, fewer dendritic silver crystals (Figure 5D) were obtained when PANI was used as an adsorbent. These results demonstrate that the PANI-EHL composite has a much more reactive sorption capacity than pure PANI, suggesting the existence of a synergistic effect in the sorption process of the PANI-EHL composite.

In addition, the average serrated length of the PANI-EHL composite is about 0.12  $\mu\text{m}$  while the average serrated length of silver ranges from 1.65 to 19.35  $\mu\text{m}$  (Figure 5B), which implies that the silver threads grow continuously and almost keep the serration of the silver threads in the process of growth. For this reason, the mechanism of crystal growth of the serrated silver most likely involves silver being generated along with the serration of the PANI-EHL composite in the initial time, shape-serrated silver threads. The serrated silver then grows bigger almost without changing the serration of the silver threads.

Furthermore, there was a great difference between the non-crystalline PANI-EHL composite (Figure 6A) and the crystalline ordered structures of the serrated threads of silver (Figure 5C). The serrated silver threads reveal four very sharp diffraction peaks at Bragg angles of 38.12, 44.30, 64.44, and 77.40°, which exactly accord with the (111), (200), (220), and (311) crystal planes of silver, as identified from the PDF Card # 65-2871, respectively.<sup>45,46</sup> For the (111) plane of silver possessing the lowest surface energy, the serrated silver threads are expected to have a preferred orientation along the (111) plane,<sup>47,48</sup> which is very likely to lead to the growth of silver threads along with hierarchical structures which show low surface and interface energy.<sup>36</sup>

The X-ray diffraction of the product of EHL after silver ion sorption is further analyzed, and found to exhibit no crystalline-



## Scheme 1. Possible Reactive Sorption Mechanism of Silver Ions onto the PANI-EHL Composite

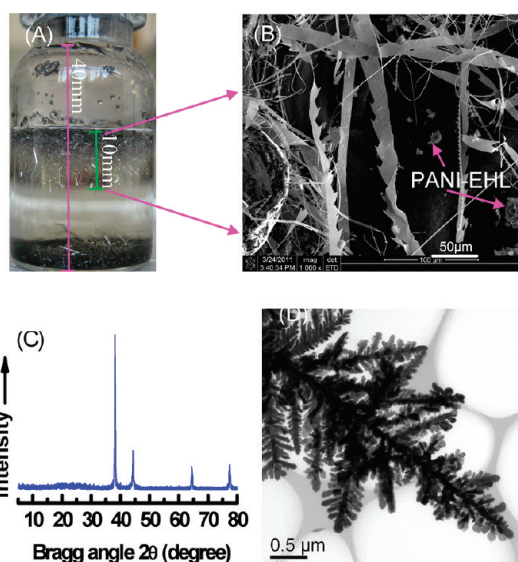
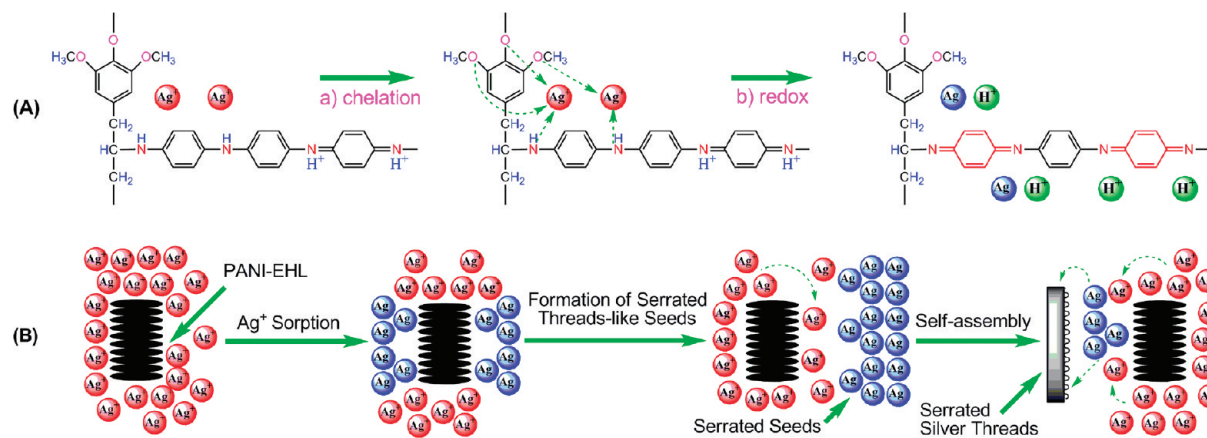


**Figure 5.** (A) Digital and (B) FE-SEM images, (C) wide-angle X-ray diffraction curve of serrated silver threads, and (D) a TEM image of the product of pure PANI after silver ion sorption.

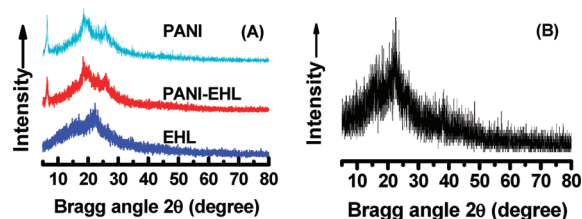


**Figure 6.** Wide-angle X-ray diffraction curves of (A) PANI, the PANI-EHL composite and EHL, and (B) the EHL sample after silver ion sorption.

ordered structures of silver crystals (Figure 6B). It can be concluded that the polycyclic structures with negative groups of EHL play a vital role in chelation rather than redox sorption. Therefore, there must be a synergistic effect that improves the reactive sorption capability of the PANI-EHL composite containing structures of PANI and EHL. This is because the oxygen-containing negative groups in EHL unit could chelate the silver ions, whereas the nitrogen-containing groups in the PANI unit could also chelate and reduce silver ions at the same time.

Generally, silver ions are sorbed by one of three types of mechanisms: physical sorption, chemical sorption, and a combination of both. The PANI-EHL composite possesses hierarchical structures and oxygen-containing negative groups, which is beneficial for reactive silver ion sorption.<sup>36,39,49</sup> Here, the surface physical sorption of silver ions onto the hierarchical composite happened first via weak van der Waals forces forming an unstable interaction between the sorbents and adsorbates.<sup>50</sup> According to the theory of hard and soft acids and bases, silver ions tend to be chelated with nitrogen and oxygen-containing functional groups, such as  $-\text{NH}_2$ ,  $-\text{NH}-$ , and  $-\text{OCH}_3$ . Therefore, the stable sorption of silver ions via chelation were gradually produced with prolonging the sorption period.<sup>49–51</sup>

During the sorption process, the  $-\text{NH}-$ ,  $-\text{NH}^+=$  and benzenoid rings of the PANI-EHL composite chains are oxidized to form  $-\text{N}=\text{}$  groups and quinoid rings, respectively, which are accompanied by the generation of silver crystals and  $\text{H}^+$  (Scheme 1A). To verify the sorption mechanism, the effect of sorption time on the pH value of the silver ion sorption solution was studied (Figure 4). The pH curve of a silver nitrate sorption solution measured over a prolonged sorption time from 0 to 36 h, showed a decline in the pH value from 3.28 to 2.64. The curve showed a sharp decline first, followed by a slow decline, and finally ending in a horizontal line. The sharp decline corresponds to the mechanism as presented above because of the many  $\text{H}^+$  produced by the redox sorption. Although the horizontal line corresponds to the sorption equilibrium of silver ions after about 22 h.

Furthermore, the mechanism of growth of the serrated silver threads is shown in Scheme 1B. The possible formation model contained three steps just as speculated above. Step 1: silver ions were quickly adsorbed onto the hierarchical PANI-EHL composite, and then the silver ions were reduced to silver nanoparticles, which was due to the inducement of the interface and the PANI-EHL composite. Step 2: the silver nanoparticles grew bigger, and then self-assembled to form serrated threads-like seeds. Once the serrated length of the serrated threadlike seeds was the same as that of the hierarchical structures of the PANI-EHL composite, the seeds departed from the surface of the composite. Step 3: the serrated threadlike seeds grew up to form serrated threads, which then continued to self-assemble with more and more reduced silver nanoparticles. In short, the silver nanoparticles self-assembled into serrated-thread seeds along with the hierarchical PANI-EHL composite in the initial

time, shaped serrated silver threads, and then continued to self-assemble almost without changing the serration of the silver threads. Compared with the hierarchical PANI-EHL composite, silver crystals could not self-assemble on the surface of pure PANI, which depended on the structure of pure PANI. Thus, silver crystals self-assembled into dendritic silver structures in acid solution.

## CONCLUSION

A hierarchical structural PANI-EHL composite has been successfully prepared using aqueous ammonia solution as a polymerization medium. The composite exhibited a strongly reactive sorption characteristic for silver ions. Serrated silver threads with length up to 10  $\mu\text{m}$  could be achieved by using the PANI-EHL composite as an adsorbent. Moreover, the PANI-EHL composite exhibited an enhanced sorption capacity than polyaniline and EHL, indicating the existence of a synergistic effect of the PANI-EHL composite between polyaniline and EHL. The effect might be due to the surface of the PANI-EHL composite carrying more acid/base sites than polyaniline and EHL. The facile preparation of the PANI-EHL composite provided an economic and effective approach to the removal and recovery of silver ions from wastewater because EHL is a low-cost and environmental material obtained from industrial and biomass waste.

## AUTHOR INFORMATION

### Corresponding Author

\*Tel: +86 591 22 866 532. Fax: +86 591 22 866 539. E-mail: qiufenglvfzu@gmail.com.

## REFERENCES

- (1) Ferry, D. K. *Science* **2008**, *319*, 579–580.
- (2) Xu, F.; Dong, C.; Xie, C.; Ren, J. *Chem.—Eur. J.* **2010**, *16*, 1010–1016.
- (3) Lasanta, T.; Olmos, M. E.; Laguna, A.; López-de-Luzuriaga, J. M.; Naumov, P. J. *Am. Chem. Soc.* **2011**, *133*, 16358–16361.
- (4) Guo, J.; Li, H.; He, H.; Chu, D.; Chen, R. *J. Phys. Chem. C* **2011**, *115*, 8494–8502.
- (5) Ma, J.; Zhang, J.; Xiong, Z.; Yong, Y.; Zhao, X. S. *J. Mater. Chem.* **2011**, *21*, 3350–3352.
- (6) Koga, H.; Kitaoka, T.; Wariishi, H. *J. Mater. Chem.* **2009**, *19*, 2135–2140.
- (7) Xu, W. P.; Zhang, L. C.; Li, J. P.; Lu, Y.; Li, H. H.; Ma, Y. N.; Wang, W. D.; Yu, S. H. *J. Mater. Chem.* **2011**, *21*, 4593–4597.
- (8) Horzum, N.; Boyacı, E.; Eroğlu, A.E.; Shahwan, T.; Demir, M.M. *Biomacromolecules* **2010**, *11*, 3301–3308.
- (9) Kononova, O.N.; Shatnykh, K.A.; Prikhod'ko, K.V.; Kashirin, D.M. *Russ. J. Phys. Chem. A* **2009**, *83*, 2340–2345.
- (10) Liao, Y.; Cao, B.; Wang, W.-C.; Zhang, L.; Wu, D.; Jin, R. *Appl. Surf. Sci.* **2009**, *255*, 8207–8212.
- (11) Kononova, O.N.; Kholmogorov, A.G.; Danilenko, N.V.; Kachin, S.V.; Kononov, Y.S.; Dmitrieva, Zh.V. *Carbon* **2005**, *43*, 17–22.
- (12) Hasany, S. M.; Ahmad, R. *Sep. Sci. Technol.* **2004**, *39*, 3509–3525.
- (13) Farag, A.B.; Soliman, M.H.; Abdel-Rasoul, O.S.; El-Shahawi, M.S. *Anal. Chim. Acta* **2007**, *601*, 218–229.
- (14) Kumar, P. A.; Chakraborty, S.; Ray, M. *Chem. Eng. J.* **2008**, *141*, 130–140.
- (15) Eisazadeh, H. *J. Appl. Polym. Sci.* **2007**, *104*, 1964–1967.
- (16) Guo, X.; Fei, G. T.; Su, H.; Zhang, L. D. *J. Phys. Chem. C* **2011**, *115*, 1608–1613.
- (17) Wang, J.; Deng, B.; Chen, H.; Wang, X.; Zheng, J. *Environ. Sci. Technol.* **2009**, *43*, 5223–5228.
- (18) Mansour, M. S.; Ossman, M. E.; Farag, H. A. *Desalination* **2011**, *272*, 301–305.
- (19) Belaib, F.; Meniai, A. H.; Bencheikh-Lehocine, M.; Mansri, A.; Morcellet, M.; Bacquet, M.; Martel, B. *Desalination* **2004**, *166*, 371–377.
- (20) Kong, Y.; Wei, J.; Wang, Z.; Sun, T.; Yao, C.; Chen, Z. *J. Appl. Polym. Sci.* **2011**, *122*, 2054–2059.
- (21) Mahanta, D.; Madras, G.; Radhakrishnan, S.; Patil, S. *J. Phys. Chem. B* **2009**, *113*, 2293–2299.
- (22) Mahanta, D.; Madras, G.; Radhakrishnan, S.; Patil, S. *J. Phys. Chem. B* **2008**, *112*, 10153–10157.
- (23) Li, X. G.; Huang, M. R.; Li, S. X. *Acta Mater.* **2004**, *52*, 5363–5374.
- (24) Li, X. G.; Liu, R.; Huang, M. R. *Chem. Mater.* **2005**, *17*, 5411–5419.
- (25) Li, X. G.; Ma, X. L.; Sun, J.; Huang, M. R. *Langmuir* **2009**, *25*, 1675–1684.
- (26) Stejskal, J.; Trchová, M.; Kovářová, J.; Prokeš, J.; Omastová, M. *Chem. Pap.* **2008**, *62*, 181–186.
- (27) Xu, P.; Jeon, S. H.; Chen, H. T.; Luo, H.; Zou, G.; Jia, Q.; Anghel, M.; Teuscher, C.; Williams, D. J.; Zhang, B.; Han, X.; Wang, H. L. *J. Phys. Chem. C* **2010**, *114*, 22147–22154.
- (28) Wu, Y.; Zhang, S.; Guo, X.; Huang, H. *Bioresour. Technol.* **2008**, *99*, 7709–7715.
- (29) Notley, S. M.; Norgren, M. *Biomacromolecules* **2008**, *9*, 2081–2086.
- (30) Harmita, H.; Karthikeyan, K. G.; Pan, X. *Bioresour. Technol.* **2009**, *100*, 6183–6191.
- (31) Acemioğlu, B.; Samil, A.; Alma, M. H.; Gundogan, R. *J. Appl. Polym. Sci.* **2003**, *89*, 1537–1541.
- (32) Crist, D. R.; Crist, R. H.; Martin, J. R. *J. Chem. Technol. Biotechnol.* **2003**, *78*, 199–202.
- (33) Liu, M. H.; Huang, J. H. *J. Appl. Polym. Sci.* **2006**, *101*, 2284–2291.
- (34) Jin, Y.; Ruan, X.; Cheng, X.; Lü, Q.-F. *Bioresour. Technol.* **2011**, *102*, 3581–3583.
- (35) Lü, Q.-F.; Huang, Z.-K.; Liu, B.; Cheng, X. *Bioresour. Technol.* **2012**, *104*, 111–118.
- (36) Zhou, C.; Han, J.; Song, G.; Guo, R. *Eur. Polym. J.* **2008**, *44*, 2850–2858.
- (37) Zhang, X.; Kolla, H. S.; Wang, X.; Raja, K.; Manohar, S. K. *Adv. Funct. Mater.* **2006**, *16*, 1145–1152.
- (38) Pan, L.; Pu, L.; Shi, Y.; Sun, T.; Zhang, R.; Zheng, Y. *Adv. Funct. Mater.* **2006**, *16*, 1279–1288.
- (39) Wang, F.; Cao, L.; Pan, A.; Liu, R.; Wang, X.; Zhu, X.; Wang, S.; Zou, B. *J. Phys. Chem. C* **2007**, *111*, 7655–7660.
- (40) Gao, Y.; Shan, D.; Cao, F.; Gong, J.; Li, X.; Ma, H. Y.; Su, Z. M.; Qu, L. Y. *J. Phys. Chem. C* **2009**, *113*, 15175–15181.
- (41) Zhou, X.; Wu, T.; Hu, B.; Yang, G.; Han, B. *Chem. Commun.* **2010**, *46*, 3663–3665.
- (42) Furukawa, Y.; Ueda, F.; Hyodo, Y.; Harada, I.; Nakajima, T.; Kawagoe, T. *Macromolecules* **1988**, *21*, 1297–1305.
- (43) Stejskal, J.; Trchová, M. *Polym. Int.* **2011**, DOI: 10.1002/pi.3179.
- (44) Šeděnková, I.; Trchová, M.; Stejskal, J.; Prokeš, J. *Appl. Mater. Interfaces* **2009**, *1*, 1906–1912.
- (45) Jin, R. H.; Yuan, J. J. *J. Mater. Chem.* **2005**, *15*, 4513–4517.
- (46) Cho, E. J.; Kang, J. K.; Han, W. S.; Jung, J. H. *Langmuir* **2008**, *24*, 5229–5232.
- (47) Kim, T. Y.; Kim, W. J.; Hong, S. H.; Kim, J. E.; Suh, K. S. *Angew. Chem. Int. Ed.* **2009**, *48*, 3806–3809.
- (48) Liang, H.; Yang, H.; Wang, W.; Li, J.; Xu, H. *J. Am. Chem. Soc.* **2009**, *131*, 6068–6069.
- (49) Huang, M. R.; Li, S.; Li, X. G. *J. Phys. Chem. B* **2010**, *114*, 3534–3542.
- (50) Li, X. G.; Feng, H.; Huang, M. R. *Chem.—Eur. J.* **2010**, *16*, 10113–10123.
- (51) Li, X. G.; Feng, H.; Huang, M. R. *Chem.—Eur. J.* **2009**, *15*, 4573–4581.

**■ NOTE ADDED AFTER ASAP PUBLICATION**

This paper was published on the Web on December 23, 2011. Reference 35 was updated, and the corrected version was reposted on December 27, 2011.